Fast Calculation of Susceptibility Weighted Imaging in Arbitrary Slice Orientation

Ryota Sato[1], Toru Shirai[1], Yo Taniguchi[1], Takenori Murase[2], and Hisaaki Ochi[1]
[1]*Hitachi, Ltd., Kokubunji, Tokyo, Japan,* [2]*Hitachi Medical Corporation, Chiba, Japan*

Target Audience: Researchers and clinicians working with or interested in quantitative susceptibility mapping (QSM) or susceptibility-weighted imaging (SWI).

Introduction:

Several approaches have recently been proposed for susceptibility-weighted imaging based on susceptibility maps instead of phase images, such as tSWI [1], a method using L1-norm regularization (Ll-SWI) [2] and susceptibility map weighted imaging (SMWI) [3]. The contrasts of susceptibility maps do not change in accordance with field direction or slice orientation while those of phase images do. Therefore, unlike conventional SWI [4], the contrasts of SWI based on susceptibility maps do not change in accordance with field direction or slice orientation [2]. However, tSWI shows non-local streaking artifacts, especially in slices parallel to the field direction [2], because of truncation in Fourier space, and L1-SWI and SMWI need long calculation time for convergence of susceptibility calculations [3]. In this study, to achieve SWI based on susceptibility maps without streaking artifacts in short calculation time, a method was developed for susceptibility-weighted imaging using a susceptibility map calculated without regularization in very small iteration number. To evaluate the usefulness of the proposed method, image contrasts in closed-type MRI and open-type MRI acquired by conventional and proposed methods were compared.

Method:

Proposed method The calculation of a susceptibility map by the least squares method takes a long time to converge. However, unlike a "quantitative" susceptibility map, which needs quantitative susceptibility values, susceptibility "weighted" imaging needs susceptibility differences between tissues and parenchyma for contrast enhancement. In the proposed method, therefore, tissue contrasts such as veins can be enhanced before convergence using an enhancement function of a susceptibility mask M as shown in Fig. 1. We call this method Susceptibility Difference Weighted Imaging (SDWI). In SDWI, first, a susceptibility map is calculated without regularization from Eq.1 using a linear conjugate gradient method.

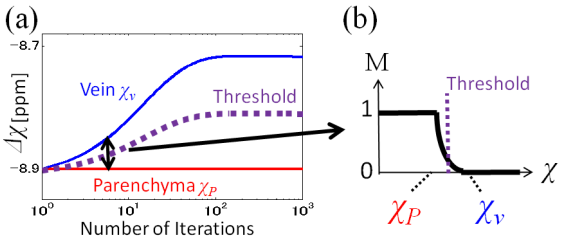

Fig. 1: Schematic views of (a) convergence process of susceptibility calculation and (b) enhancement function.

$$\chi = \mathrm{argmin}_{\chi} \| \mathbf{W}(\varphi - C\chi) \|_2^2 \quad , \qquad (1)$$

where W denotes a weight derived from the phase image, φ denotes a phase image, χ denotes a susceptibility map, and C denotes a matrix representing a convolution with unit dipole magnetic field. There are only three iterations (the calculation time is about 20 seconds using a PC with 3.0GHz CPU). Second, a susceptibility mask M(i) is calculated from susceptibility $\chi(i)$ by using a threshold χ_M as shown in our previous work [2]. Lastly, the susceptibility mask M is multiplied to the absolute image. *Experiments* To compare the image contrasts of the conventional and proposed methods, SWI, tSWI, and SDWI were applied to measurements of healthy volunteers. Experiments were performed on a 1.5T closed-type MRI and 1.2T open-type MRI. The scan parameters in all experiments were as follows: Sequence: RSSG-EPI (RF spoiled-steady state acquisition with rewound gradient echo - echo planar imaging); TR/effective TE = 65/40 ms (closed-type MRI) and 80/40 ms (open-type MRI); NSA = 2; FA = 25; matrix: 512×384×40; reconstruction matrix: 512×512×80; and FOV: 220×220×80 mm. *Processing* After the low-spatial-frequency components of the background phase were removed by performing high-pass filtering for each slice, noise in the air region in the phase image was removed by thresholding. This preprocessed phase image was processed by SWI [1], tSWI [2], and SDWI. In the case of tSWI, a k-space truncation value, $\chi_{M,}$, and n were set to 0.1, 0.8 ppm, and 4, respectively [1]. For all methods, minimum intensity projection (minIP) was carried out over 15 mm around red nuclei. *Evaluation* Image contrasts of axial slices in closed-type MRI and axial slices in open-type MRI acquired by SWI [1], tSWI [2], and SDWI were compared. The axial slices in closed-type MRI are perpendicular to the field direction, and the axial slices in open-type MRI are parallel to the field direction.

Results and Discussion:

As shown in Fig. 2(a)-(c), in the case of an axial slice in closed-type MRI, SDWI can visualize veins (yellow arrows) and iron depositions (red arrows) as accurately as SWI and tSWI can, and SDWI shows less background inhomogeneity than SWI and tSWI (blue arrows). As shown in Fig. 3(a), in the case of an axial slice in open-type MRI, SWI does not enhance veins (yellow arrows) or iron depositions (red arrows) clearly. As shown in Figure 3(b), streaking artifacts (green arrows) and shading (blue arrows) are observed in the case of tSWI. As shown in Figure 3(c), SDWI enhances contrast of veins (yellow arrows) and iron depositions (red arrows) without causing artifacts. These results confirm that SDWI can enhance contrast without streaking artifacts regardless of slice orientation, while SWI cannot enhance contrast clearly and tSWI shows streaking artifacts in slice parallel to the field direction.

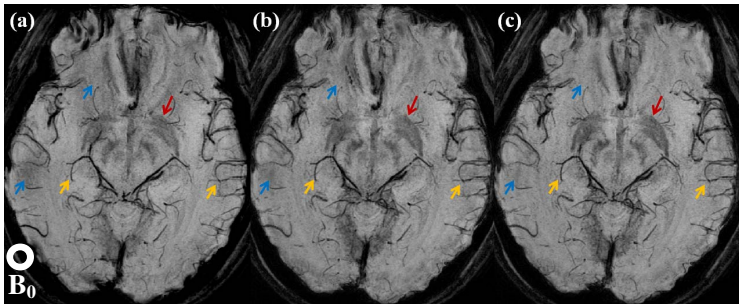

Fig. 2: Axial images in closed-type MRI by (a) SWI, (b) tSWI, and (c) SDWI.

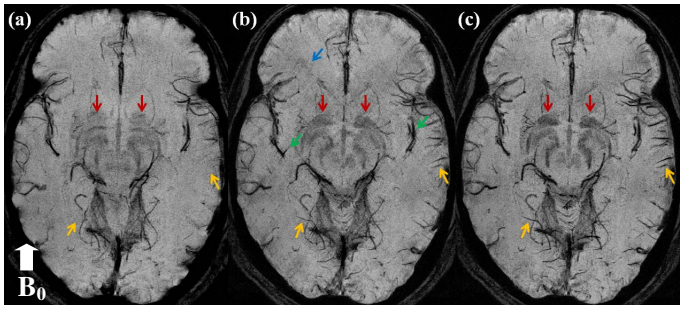

Fig. 3: Axial images in open-type MRI by (a) SWI, (b) tSWI, and (c) SDWI.

Conclusion:

The results suggest that SDWI can enhance contrast of regions with high magnetic susceptibility, such as veins or iron depositions, in arbitrary slice orientation within a short calculation time without streaking artifacts.

References: [1] Mok et al. ISMRM 2012; 2366 [2] Sato et al. ISMRM 2013; 2480 [3] Gho et al. MRM 2013 *in press*. [4] Haacke et al. MRM 2004; 52:612